Proceedings of Science and Mathematics
Faculty of Science, Universiti Teknologi Malaysia
Vol. 10, 2022, page 176 – 187

Modelling of the Transmission of Tuberculosis Using SEIR Model

Muhamad Aidid Danial Ahmad Kusairi, Ang Tau Keong*, Fuaada Mohd Siam
Department of Mathematical Sciences, Faculty of Science, Universiti Teknologi Malaysia
*Corresponding author: taukeong@utm.my

Abstract
Tuberculosis (TB) is caused by a bacterium called Mycobacterium tuberculosis. Tuberculosis is mostly found in the lungs, although they can also be found in the kidney, spine, and brain. The goal of this study is to investigate the dynamics of influenza transmission using the Susceptible – Exposed – Infected - Recovered (SEIR) model, which is based on the compartmental dynamics of infectious diseases. The SEIR model is based on the system of Ordinary Differential Equations (ODEs). The model contains two non-negative equilibria which are the disease-free equilibrium and endemic equilibrium. The stability properties of the proposed model are determined by the Routh-Hurwitz criterion. The basic reproductive number, R_0, is calculated using the Next-Generation Matrix Method. It is acknowledged that when $R_0 < 1$, the disease does not spread. The simulations of tuberculosis transmission are investigated using the ODE45 in MATLAB built-in tool. The values of certain parameters are changed and compared to learn the effects of the outcome. Hence, the findings can be used to prevent the spread of tuberculosis in the population.

Keyword:

1. Introduction

Tuberculosis (TB) is a communicable disease that is a major cause of illness, one of the top ten causes of death globally and the leading cause of death from a single infectious agent. In 2019, approximately 10 million people were diagnosed with tuberculosis (TB) and 1.4 million died because of the disease. Tuberculosis is caused by the bacillus Mycobacterium tuberculosis [1, 2], which is spread when people with tuberculosis expel bacteria into the air, such as when coughing [3, 4]. The disease most commonly affects the lungs (pulmonary tuberculosis), but it can also affect other organs (extrapulmonary tuberculosis) [5, 6, 7]. Tuberculosis can affect anyone and anywhere but most people who develop the disease (about 90%) are adults; men have more cases than women; and 87 percent of those who became ill with tuberculosis in 2019 were in one of 30 high tuberculosis burden countries [8]. Nationally, case rates range from less than 5 to more than 500 per 100,000 population per year [9]. People affected by tuberculosis often face economic hardship, vulnerability, marginalization, stigma, and discrimination because the disease is a disease of poverty. Mycobacterium tuberculosis infects about a quarter of the population of the world.

Tuberculosis is both curable and preventable. Most people (approximately 85 percent) who develop tuberculosis can be successfully treated with a 6-month drug regimen. Treatment can serve as an added benefit of preventing infection transmission [10, 11, 12]. Since 2000, tuberculosis treatment has saved over 60 million lives [9], but with access still falling short of Universal Health Coverage (UHC), many millions have missed out on diagnosis and care. People infected with tuberculosis can receive preventive treatment. The number of people developing infection and disease which leads to death can also be reduced through multisectoral action to address tuberculosis determinants such as poverty, malnutrition, HIV infection, and diabetes [13, 14].

Understanding the dynamics of tuberculosis disease transmission can help to avoid and control the spread of the epidemic as the disease grows more severe. The dynamical transmission behaviour of the tuberculosis illness will be discussed in this study to make use of the mathematical modelling approach known as the Susceptible- Exposed-Infected-Removed (SEIR) epidemiological modelling. Tuberculosis primarily affects adults in their prime years of life [15]. However, all age groups are at risk. Over 95 percent of cases and deaths occur in developing countries [16, 17, 18].

The mathematical approach to this pandemic is also an important step in minimising tuberculosis spread. The Susceptible - Exposed - Infected - Recovered (SEIR) model is one example of mathematical modelling that can be used to understand the dynamics of tuberculosis illness. As a result, the dynamics of illness transmission may be comprehended. Certain viable techniques for reducing the impact of the tuberculosis epidemic may be presented. The significance of this study is to help us understand how tuberculosis outbreaks spread. The value of parameters might be predicted based on previous research on infectious disease. We can control it by changing the values of certain parameters. The pandemic tuberculosis can then be predicted by calculating the basic reproduction number, R_0, at the equilibrium points. The findings can be used to control the spread of the pandemic.

2. Literature Review

2.1. SEIR Model

This section briefly discussed the derivation of extended SIR model for the pandemic of tuberculosis. The extended SIR model is called as Suspected-Exposed-Infected-Recovered (SEIR) model. The SEIR model derivation and the stability analysis of the model will be carried out throughout this section. Also, the Next-Generation Matrix method is employed to obtain the basic reproduction number and the local stability of the tuberculosis distribution model is carried out [19].

The SEIR model is used to compute the number of infected, recovered, and dead individuals based on the number of contacts, probability of disease transmission, incubation, and infectious periods as well as disease fatality rate. SEIR is one of the most used mathematical algorithms to describe the spread of an epidemic disease. The SEIR model is predicated based on the following biological assumptions [19]:

1. A person can become infected simply by coming into contact with irresistible individuals.
2. The likelihood of an individual being tainted is unaffected by age, sex, societal position, race and climatic conditions.
3. The passing rate is thought to be consistent across all hosts, and the total number of passings is adjusted by complete enlistment, resulting in a consistent population.
4. Individuals have the same level of interaction with one another.
5. The disease spreads in a small area, implying that there is no emigration or immigration, as well as no births or deaths in the population. As a result, the total number of individuals in the population N remains constant.
6. The natural death rate in each compartment is the same.

The SEIR model considers a population of size N in which, at time t, S individuals are susceptible to infection, E is the exposed, I individuals being infected and capable of transmitting or spreading the disease to the susceptible population. R represents the number of people who have recovered from the disease. This includes people who have died and cannot be infected again. The behaviour of the disease is based on the 1930s work of Kermack and Kendrick [35]. Total population size by $N(t)$ is as follows:

$$N\,(t) = S(t) + E\,(t) + I\,(t) + R(t) \quad (1)$$

Table 1. Parameters and the definitions

Parameter	Definition

β	Rate of contact of effective contacts with other susceptible individuals
ε	Rate at which the exposed individuals become infective
γ	Recovery rate
μ	Birth and death rate

$$\frac{dS}{dt} = \mu N - \mu S - \beta SI, \quad (2)$$

$$\frac{dE}{dt} = \beta SI - (\mu + \varepsilon)E, \quad (3)$$

$$\frac{dI}{dt} = \varepsilon E - (\mu + \gamma)I, \quad (4)$$

$$\frac{dR}{dt} = \gamma I - \mu R. \quad (5)$$

The nonlinear system of differential equations has the initial conditions

$S(0) = S_0 > 0, E(0) = E_0 > 0, I(0) = I_0 > 0$ and $R(0) = R_0 > 0$. (6)

The contact rate, the infection rate, the recovery rate and the birth and death rate are all non-negative ($\beta > 0, \varepsilon > 0, \gamma > 0$, and $\mu > 0$ respectively. Thus, $N(t) = S(t) + E(t) + I(t) + R(t)$ and

$$\frac{dS}{dt} + \frac{dE}{dt} + \frac{dI}{dt} + \frac{dR}{dt} = 0. \quad (7)$$

2.2. Formulation of basic reproductive number, R_0, for tuberculosis

Basic reproduction number, R_0 is the expected number of cases caused by a single case in a population where all individuals are susceptible to infection. The values of R_0 can be one of the three things [20]:

1. The basic reproduction number represents the average number of new infections for each infected person. The greater the R_0 value, the faster the disease spreads, and the lower the R_0 value, the slower the disease spreads.
2. $R_0 < 1$ means the cases are stable.
3. $R_0 > 1$ means the outbreak is self-sustaining unless effective control measures are implemented.

Use the equations (3) - (4) to apply the next generation matrix method to determine the basic reproductive number. The basic reproductive number, R_0, is

$$R_0 = \frac{\beta\varepsilon}{(\mu+\varepsilon)(\mu+\gamma)}. \quad (8)$$

3. Methodology

3.1. Existence of Equilibrium Points

The model has two equilibrium points called disease-free equilibrium and endemic equilibrium. For obtaining the equilibrium points, the above differential equations should be equated to zero. Thus, the equations can be written as

$$\frac{dS}{dt} + \frac{dE}{dt} + \frac{dI}{dt} + \frac{dR}{dt} = 0, \quad (9)$$

$$\mu - (\mu + \beta I)S = 0, \quad (10)$$

$$\beta SI - (\mu + \varepsilon)E = 0, \quad (11)$$

$$\varepsilon E - (\mu + \gamma)I = 0. \quad (12)$$

3.2. Disease-Free Equilibrium Points

In a disease-free equilibrium, the population is free from disease and consequently $I = 0$, we get

$S = 1$ and $E = 0$. Hence, the equilibrium point for the disease-free equilibrium is given as:

$$(S^*, E^*, I^*, R^*) = (1, 0, 0, 0). \quad (13)$$

3.3. Endemic Equilibrium Points

The Endemic Equilibrium state indicates that the infection is still present in the structure. The endemic equilibrium point will be determined at $i \neq 0$. Equations (10) − (12) can be solved to obtain the values of S, E, I and R. Let Se, Ee, Ie and R_e to represent the endemic equilibrium points for the respective states. The endemic equilibrium points for the respective states are as follows:

$$S_e, E_e, I_e, R_e = \left(\frac{1}{R_0}, \frac{\mu R_0 - 1}{(\mu+\varepsilon)R_0}, \frac{\mu R_0 - 1}{\beta}, \frac{\gamma(\mu R_0 - 1)}{\beta\mu}\right). \quad (14)$$

3.4. Stability Analysis at Disease-Free Equilibrium Points (DFEP)

The Jacobian matrix for the Disease-Free equilibrium is given by

$$J(S^*, E^*, I^*, R^*) = \begin{pmatrix} -\mu - \beta I & 0 & -\beta S & 0 \\ \beta I & -\mu - \varepsilon & \beta S & 0 \\ 0 & \varepsilon & -\mu - \gamma & 0 \\ 0 & 0 & \gamma & -\mu \end{pmatrix}. \quad (15)$$

Evaluate the Jacobian matrix at the equilibrium points $(S^*, E^*, I^*, R^*) = (1, 0, 0, 0)$ to get:

$$J(S^*, E^*, I^*, R^*) = \begin{pmatrix} -\mu & 0 & -\beta & 0 \\ 0 & -\mu - \varepsilon & \beta & 0 \\ 0 & \varepsilon & -\mu - \gamma & 0 \\ 0 & 0 & \gamma & -\mu \end{pmatrix}. \quad (16)$$

Solving for roots of the characteristic polynomial given in the Jacobian matrix leads to the characteristic equation given as:

$$f(\lambda) = a_0\lambda^4 + a_1\lambda^3 + a_2\lambda^2 + a_3\lambda + a_4, \quad (17)$$

Where

$$a_0 = 1, \quad (18)$$

$$a_1 = 4\mu + \gamma + \varepsilon, \quad (19)$$

$$a_2 = -\beta\varepsilon + 6\mu^2 + 3\mu\gamma + 3\varepsilon\mu + \varepsilon\gamma, \quad (20)$$

$$a_3 = -2\varepsilon\mu\beta + 4\mu^3 + 3\mu^2\gamma + 3\varepsilon\mu^2 + 2\varepsilon\mu\gamma, \quad (21)$$

$$a_4 = -\varepsilon\mu^2\beta + \mu^4 + \mu^3\gamma + \varepsilon\mu^3 + \varepsilon\mu^2. \quad (22)$$

By Routh-Hurwitz Criterion, diseases-free equilibrium is stable if $a1 > 0, a3 > 0$ and $a1a2 - a3 > 0$. From equation (17), obviously $a_1 > 0$ and $a_3 > 0$ if $4\mu^3 + 3\mu^2\gamma + 3\varepsilon\mu^2 + 2\varepsilon\mu\gamma > 2\varepsilon\mu\beta$
If in accordance with those conditions, this means that the system is locally asymptotically stable.

3.5. Stability Analysis at Endemic Equilibrium Points (EEP)

The endemic stable state has equilibrium point in term of R_0 in equation (3.6) given by:

$$S_e, E_e, I_e, R_e = \left(\frac{1}{R_0}, \frac{\mu R_0 - 1}{(\mu+\varepsilon)R_0}, \frac{\mu R_0 - 1}{\beta}, \frac{\gamma(\mu R_0 - 1)}{\beta\mu}\right). \quad (23)$$

The Jacobian matrix is given by

$$J(S^*, E^*, I^*, R^*) = \begin{pmatrix} -\mu R_0 & 0 & -\frac{\beta}{R_0} & 0 \\ \mu R_0 - 1 & -\mu - \varepsilon & \frac{\beta}{R_0} & 0 \\ 0 & \varepsilon & -\mu - \gamma & 0 \\ 0 & 0 & \gamma & -\mu \end{pmatrix}.$$

(24)

Solving for roots of the characteristic polynomial given in the Jacobian matrix leads to the characteristic equation given as:

$$f(\lambda) = b_0\lambda^4 + b_1\lambda^3 + b_2\lambda^2 + b_3\lambda + b_4, \quad (25)$$

Where

$b_0 = 1,$ (26)

$b_1 = R_0\mu + 2\mu + \gamma + \varepsilon + \mu,$ (27)

$b_2 = 2R_0\mu^2 + R_0\mu\gamma + \varepsilon R_0\mu + R_0\mu^2 + 2\mu^2 + \gamma\mu + \varepsilon\mu,$ (28)

$b_3 = R_0\mu^3 + R_0\mu^2\gamma + \varepsilon R_0\mu\gamma - \mu^2 - \mu\gamma - \varepsilon\mu - \varepsilon\gamma + 2R_0\mu^3 + R_0\mu^2 + \varepsilon R_0\mu,$ (29)

$b_4 = R_0\mu^4 + R_0\mu^3\gamma + \varepsilon R_0\mu^2\gamma - \mu^3 - \mu^2\gamma - \varepsilon\mu^2 - \mu\varepsilon\gamma.$ (30)

Based on Routh-Hurwitz stability criterion, endemic equilibrium is stable if $b_1 > 0, b_3 > 0$, and $b_1 b_2 - b_3 > 0$. If in accordance with those conditions, this means that the system is locally asymptotically stable.

4. Results and Discussion

4.1. Result of Simulations of the SEIR Model

To perform numerical simulation, we adopt the parameter values that are chosen and modified from the reference [19].

Table 2. Parameters and their estimated values used in the model.

Parameter	Estimated Value
μ	0.001
β	0.25
ε	0.15
γ	0.1

The result of simulation of the SEIR model for the parameter values is shown in Figure 1.

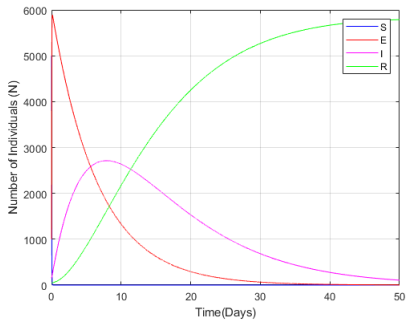

***Figure* 1** Simulation of the SEIR model for $\beta = 0.25, \varepsilon = 0.15, \gamma = 0.1, \mu = 0.001.$

Figure 1 depicts the combination of graphs from the four classes: S, E, I, and R. These figures will be used as the foundation for comparing and observing changes in parameter values, β, ε and γ. Figure 1 depicts the graph of all four classes of SEIR model with initial parameters of $\beta = 0.25, \varepsilon = 0.15, \gamma = 0.1$, and $\mu = 0.001$.

4.2. Changes in β

In this section, the value of rate of contact, β is changed to observe the spread of tuberculosis in a population. The rate of contact, β varies from 0.25 to 0.5 and then 0.75. The remaining parameters are the same where $\mu = 0.001, \varepsilon = 0.15$ and $\gamma = 0.1$.

Figure 2 - Figure 5 display the curves for each compartment separately in each figure. The following results are analysed by comparing the curves to the base model. As shown in the generated figures, the changes of the value β does not change the direction and shape compared to the original graph where $\beta = 0.25$. However, there is a very slight to none difference in the generated zoomed in graph of each susceptible, exposed, infected and recovered graphs. This shows that the rate of contact, β does not play a significant role in the compartmental tuberculosis model.

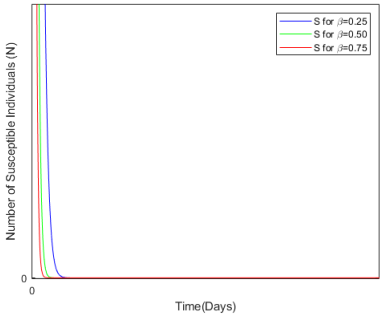

Figure 2 Variation in the number of Susceptible populations, (S) for different β values.

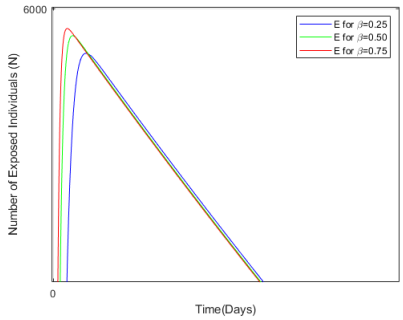

Figure 3 Variation in the number of Exposed populations, (E) for different β values.

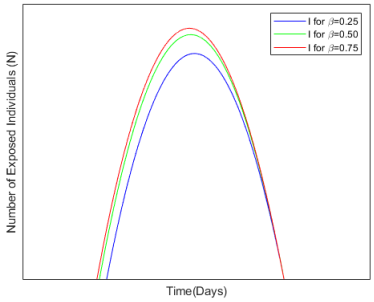

Figure 4 Variation in the number of Infected populations, (I) for different β values.

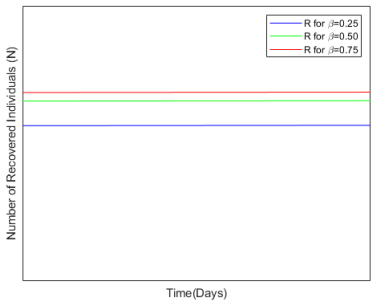

Figure 5 Variation in the number of Recovered populations, (R) for different β values.

In Figure 2, the curve with the highest β value which is $\beta = 0.75$ flattens faster compared to the curve with $\beta = 0.50$ and $\beta = 0.25$ respectively. This means that the higher the rate of contact, β, the faster it took to flatten the susceptible population curve.

In Figure 3, the E curve for $\beta = 0.75$ reach the highest peak compared to the $\beta = 0.50$ and $\beta = 0.25$ respectively. However, the highest β value curve of the exposed individuals curve flattens earlier compared to the lower β. This means that the higher the rate of contact of effective contacts with other susceptible individuals, β, the higher the number of exposed individuals. Besides that,it is also means that the higher the rate of contact of effective contacts with other susceptible individuals, the faster the the exposed population curve to flatten.

In Figure 4, the infected population curve for $\beta = 0.75$ which is the highest β value reach the highest peak compared to the $\beta = 0.50$ and $\beta = 0.25$ respectively. After reaching the peak , every exposed population curves with different values of β began to dive in, eventually reaching the same population as the curve with the initial value of $\beta = 0.25$. This conclude that the higher the rate of contact of effective contacts with other susceptible individuals, the higher the number of infected individuals.

Based on Figure 5, every recovered population curves grew steadily until the $50th$ day. The highest rate of contact, $\beta = 0.75$ produce the the highest number of recovered individuals compared to the curves with $\beta = 0.5$ and $\beta = 0.25$ respectively. This means that the higher the rate of contact of effective contacts with other susceptible individuals, the higher the number of recovered individuals in the population.

4.3. Changes in ε

The rate at which exposed individuals become infected, ε varied with different ε values: $0.15, 0.3$ and 0.45. The remaining values of the parameters are the same as the basis simulation: $\mu = 0.001, \beta = 0.25$ and $\gamma = 0.1$. Figure 6 – Figure 9 represent the population curve for each compartment.

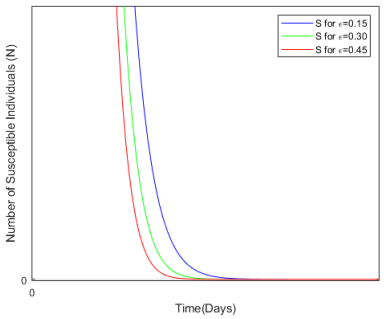

Figure 6 Variation in the number of Susceptible populations, (S) for different ε values.

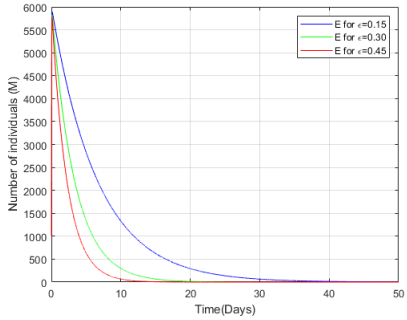

Figure 7 Variation in the number of Exposed populations, (E) for different ε values.

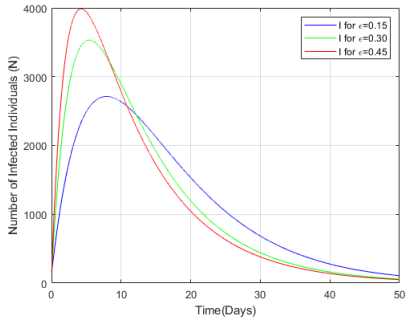

Figure 8 Variation in the number of Infected populations, (I) for different ε values.

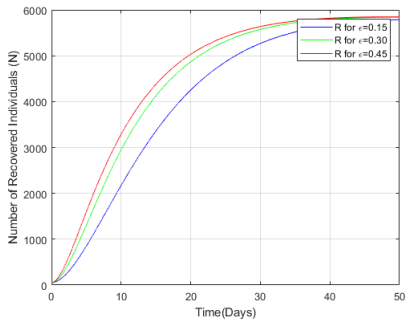

Figure 9 Variation in the number of Recovered populations, (R) for different ε values.

Figure 6 displays the susceptible population curves for various ε values. As can be seen, the susceptible population curve with the highest ε value, $\varepsilon = 0.45$ flattens quicker compared to the lower ε values. This means that the higher the rate at which the exposed individuals become infective, the quicker it take to flatten the number of susceptible population curve.

Figure 7 illustrates the exposed population curves for various ε values. Based on the population curves, every ε reached the peak at almost 6000 individuals. After that, the curves decline rapidly at

between day 0 and day 10. As can be seen, the value of $\varepsilon = 0.15$ decline slower as compared to $\varepsilon = 0.3$ and $\varepsilon = 0.45$. This conclude that the lower the rate at which the exposed individuals become infective, the lesser the exposed individuals per unit time.

Based on Figure 8, every infected population curves, I, showed significant variations as the rate at which the exposed individuals become infected. When the value of parameter $\varepsilon = 0.45$, the infected population curve grew rapidly until it hits the peak of over 2500 individuals infected. After that, the curve begin to dive in, eventually reaching the same infected population curve with $\varepsilon = 0.15$ and $\varepsilon = 0.3$. Increasing rate at which the exposed individuals become infective, ε would result in higher infected individuals per unit time.

Based on Figure 9, every recovered population curves, R, showed significant variations as the rate at which the infected individuals become infected was increasing steadily until it reach the limit of almost 6000 individuals. The higher the rate at which the exposed individuals become infective the higher the peak of the recovered population curve. $\varepsilon = 0.45$ reached the highest peak at almost 6000 individuals. Once the curves reached the highest peak, the curve begins to decline slightly with time.

4.4. Changes in γ

The rate at which the infected individuals recover, γ varied with different γ values: $0.1, 0.2$ and 0.4. The remaining values of the parameters are the same as the basis simulation: $\mu = 0.001, \beta = 0.25$ and $\varepsilon = 0.15$. Figure 10 - Figure 13 represent the population curve for each compartment.

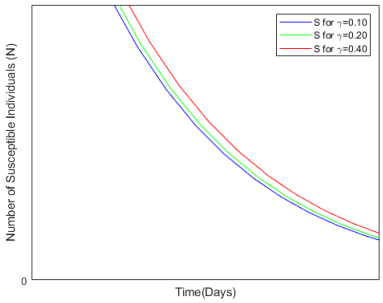

Figure 10 Variation in the number of Susceptible populations, (S) for different γ values.

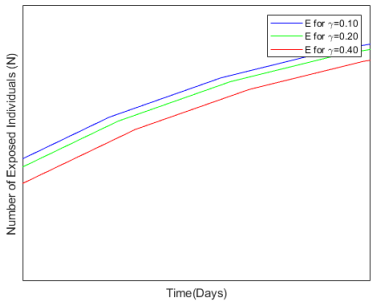

Figure 11 Variation in the number of Exposed populations, (E) for different γ values

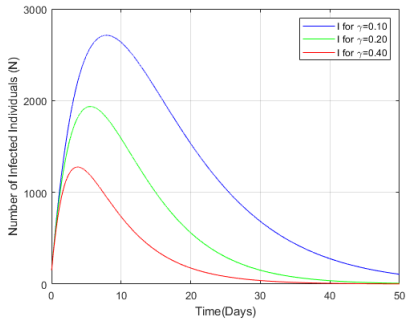

Figure 12 Variation in the number of Infected populations, (I) for different γ values.

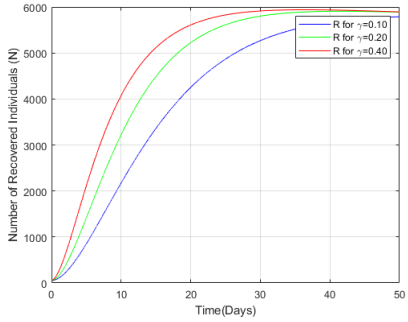

Figure 13 Variation in the number of Recovered populations, (R) for different γ values.

Figure 10 illustrates the susceptible population curves for various γ values. The susceptible population curve with $\gamma = 0.40$ which is the highest took a longer time to flatten the curve compared to the $\gamma = 0.2$ and $\gamma = 0.1$ respectively. This means that, the higher the value of γ of the susceptible population curve, the higher the time it took to flatten the curve. This means that the higher the rate at which the infected individuals recover, the longer it took for the number of susceptible population curve to flatten.

Figure 11 illustrates the exposed population curves for various γ values. As can be seen, the highest value of γ which is $\gamma = 0.4$ reach the highest peak of the exposed population curve compared to the $\gamma = 0.2$ and $\gamma = 0.1$ respectively. All the curves later continue to decline over time until zero exposed individuals. The curve with the highest γ value also took a longer time to flatten compared to the lower value of γ. This means that the higher the rate at which the infected individuals recover, γ, the higher the number of exposed individuals and the longer it took to flatten the exposed population curve.

Based on Figure 12, every infected population curve, I, showed significant variations as the rate at which the infected individuals recover was increasing and decreasing between day 0 and day 10. The number of infected individuals with the smallest value of γ reach the highest peak at almost 3000 individuals compared to the infected population curves with the values of $\gamma = 0.2$ and $\gamma = 0.4$. This conclude that the smaller the rate at which the infected individuals recover, the higher the number of infected individuals in the population curve. In addition, the higher the rate at which the exposed individuals become infected, ε, the faster it took to flatten the infected population curve.

Based on Figure 13, every recovered population curve, R, showed significant variations as the rate at which the infected individuals recover was increasing steadily until it reaches the limit of more than 5000 individuals. The recorded population at $\gamma = 0.4$ which is the highest γ reached the highest peak at almost 6000 individuals. The higher the rate at which the infected individuals recover, the higher the peak of the recovered population curve. Once the curves reached the highest peak, the curve begins to decline slightly with time.

Conclusion

The SEIR compartmental model is used to explore the transmission of pandemic tuberculosis. The SEIR model is a development of the commonly used SIR model in infectious disease research. A few

assumptions were made to make the model more feasible for real-world applications. The equilibrium points of the ODEs system were calculated using the SEIR model.

In this SEIR model, the influence of modifying the parameter values is observed and analysed. To simulate graphs with a few alternative values for each of the parameters, ODE45 MATLAB software was used. According to the simulation results, one parameter to be consider in preventing tuberculosis transmission is the infection rate. By teaching people about the spread of infection, the rate of infection can be reduced. Apart from that, the rate of recuperation should be boosted. Wearing a face mask, avoiding crowded areas, and practising social distancing and avoiding intimate contact with infected people are all recommended to increase the recovery rates.

Based on the study findings, the SEIR model can be used as a reference model for tuberculosis spread. The model analysis provides an overview of local stability in the spread of tuberculosis. The findings can be used to guide early tuberculosis pandemic prevention efforts.

Acknowledgement

A final year project report submitted in partial fulfilment of the requirements for the award of the degree of Bachelor of Science (Industrial Mathematics). This project would not have been possible without the support of many people. Many thanks to my supervisors, Dr. Ang Tau Keong and Dr. Fuaada Mohd Siam, who read my numerous revisions and helped me identify the mistakes I made. Also, thanks to my friends, who are always there in difficult and happy times throughout our journey in finishing this degree.

References

[1] Tang, J., Yam, W.-C. and Chen, Z. Mycobacterium tuberculosis infection and vaccine development. Tuberculosis, 2016. 98: 30–41. [2] Bicego, M., Acosta-Muñoz, C., Orozco-Alzate, M. 2013. Classification of Seismic Volcanic Signals Using Hidden-Markov-Model-Based Generative Embeddings. *IEEE Transactions on Geoscience and Remote Sensing,* 51: 3400-3409.

[2] Lee, S. H. Tuberculosis Infection and Latent Tuberculosis. Tuberculosis and Respiratory Diseases, 2016. 79(4): 201-206.

[3] Singer-Leshinsky, S. Pulmonary tuberculosis: Improving diagnosis and management. Journal of the American Academy of Physician Assistants, 2016. 29(2): 20–25.

[4] Faizal, I. A., Pangesti, I. and P, D. A. S. House Environments As Risk Factors Of Tuberculosis In Cilacap District. Jurnal Riset Kesehatan, 2021. 10(1): 65–70.

[5] Gambhir, S., Ravina, M., Rangan, K., Dixit, M., Barai, S. and Bomanji, J. Imaging in extrapulmonary tuberculosis. International Journal of Infectious Diseases, 2017. 56: 237-247.

[6] Rodriguez-Takeuchi, S. Y., Renjifo, M. E. and Medina, F. J. Extrapulmonary Tuberculosis: Pathophysiology and Imaging Findings. RadioGraphics, 2019. 39(7): 2023–2037.

[7] Qian, X., Nguyen, D. T., Lyu, J., Albers, A. E., Bi, X. and Graviss, E. A. Risk factors for extrapulmonary dissemination of tuberculosis and associated mortality during treatment for extrapulmonary tuberculosis. Emerging Microbes & Infections, 2018. 7(1): 1–14.

[8] Global tuberculosis report 2019. URL https://www.who.int/publications-detail-redirect/9789241565714.

[9] Global tuberculosis report 2021. URL https://www.who.int/publications-detail-redirect/9789240037021.

[10] Velayutham, B., Chadha, V. K., Singla, N., Narang, P., Rao, V. G., Nair, S., Ramalingam, S., Sivaramakrishnan, G. N., Joseph, B., Selvaraju, S., Shanmugam, S., Narang, R., Pachikkaran, P., Bhat, J., Ponnuraja, C., Bhalla,
B.B., Shivashankara, B. A., Sebastian, G., Yadav, R., Sharma, R. K., Sarin, R., Myneedu, V. P., Singla, R., Khayyam, K., Mrithunjayan, S. K., Jayasankar, S. P., Sanker, P., Viswanathan, K., Viswambharan, R., Mathuria, K., Bhalla, M., Singh, N., Tumane, K. B., Dawale, A., Tiwari, C. P., Bansod, R., Jayabal, L., Murali, L., Khaparde, S. D., Rao, R., Jawahar, M. S. and Natrajan, M. Recurrence of tuberculosis among newly diagnosed sputum positive pulmonary tuberculosis

patients treated under the Revised National Tuberculosis Control Programme, India: A multi-centric prospective study. PLOS ONE, 2018. 13(7).

[11] Bastos, M. L., Lan, Z. and Menzies, D. An updated systematic review and meta-analysis for treatment of multidrug-resistant tuberculosis. European Respiratory Journal, 2017. 49(3).

[12] Atif, M., Bashir, A., Ahmad, N., Fatima, R. K., Saba, S. and Scahill, S. Predictors of unsuccessful interim treatment outcomes of multidrug resistant tuberculosis patients. BMC Infectious Diseases, 2017. 17(1): 655.

[13] Glaziou, P., Floyd, K. and Raviglione, M. C. Global Epidemiology of Tuberculosis. Seminars in Respiratory and Critical Care Medicine, 2018. 39(3): 271–285. [15]Walpole, R. E., Myers, R. H., Myers, S. L, Ye, K. 2012. Probability & Statistics for Engineers & Scientist, 9th ed. Pearson Education, Inc., Boston.

[14] Floyd, K., Glaziou, P., Zumla, A. and Raviglione, M. The global tuberculosis epidemic and progress in care, prevention, and research: an overview in year 3 of the End TB era. The Lancet Respiratory Medicine, 2018. 6(4): 299–314.

[16] Whittaker, E., López-Varela, E., Broderick, C. and Seddon, J. A. Examining the Complex Relationship Between Tuberculosis and Other Infectious Diseases in Children. Frontiers in Pediatrics, 2019. 7.

[16] Ali, M. K., Karanja, S. and Karama, M. Factors associated with tuberculosis treatment outcomes among tuberculosis patients attending tuberculosis treatment centres in 2016-2017 in Mogadishu, Somalia. Pan African Medical Journal, 2017. 28(1).

[17] Amere, G. A., Nayak, P., Salindri, A. D., Narayan, K. M. V. and Magee, M. J. Contribution of Smoking to Tuberculosis Incidence and Mortality in High-Tuberculosis-Burden Countries. American Journal of Epidemiology, 2018. 187(9): 1846-1855.

[18] Bogale, S., Diro, E., Shiferaw, A. M. and Yenit, M. K. Factors associated with the length of delay with tuberculosis diagnosis and treatment among adult tuberculosis patients attending at public health facilities in Gondar town, Northwest, Ethiopia. BMC Infectious Diseases, 2017. 17(1): 145.

[19] Das, K., Murthy, B. S. N., Samad, S. A. and Biswas, M. H. A. Mathematical transmission analysis of SEIR tuberculosis disease model. Sensors International, 2021. 2: 100120.

[20] Locatelli, I., Trächsel, B. and Rousson, V. Estimating the basic reproduction number for COVID-19 in Western Europe. PLOS ONE, 2021. 16(3): e0248731.